water

MDPI

Article

Electrochemical Recovery to Overcome Direct Osmosis Concentrate-Bearing Lead: Optimization of Treatment Process via RSM-CCD

Milaad Moosazade [1], Razieh Ashoori [2], Hamid Moghimi [3], Mohammad Ali Amani [4], Zacharias Frontistis [5] and Ramezan Ali Taheri [1,*]

1 Nanobiotechnology Research Center, Baqiyatallah University of Medical Sciences, Tehran 14351-16471, Iran; milaadmoosazade2022@gmail.com
2 Department of Environmental Health Engineering, School of Health, Shiraz University of Medical Sciences, Shiraz 71348-14336, Iran; ra.ashoori90@gmail.com
3 Department of Microbial Biotechnology, School of Biology, College of Science, University of Tehran, Tehran 14155-6455, Iran; hmoghimi@ut.ac.ir
4 Applied Biotechnology Research Center, Baqiyatallah University of Medical Sciences, Tehran 14351-16471, Iran; rsr.amani@bmsu.ac.ir
5 Department of Chemical Engineering, University of Western Macedonia, GR-50132 Kozani, Greece; zfrontistis@uowm.gr
* Correspondence: taheri@bmsu.ac.ir

Abstract: The use of electrochemistry is a promising approach for the treatment of direct osmosis concentrate that contains a high concentration of organic pollutants and has high osmotic pressure, to achieve the safe discharge of effluent. This work addresses, for the first time, this major environmental challenge using perforated aluminum electrodes mounted in an electrocoagulation–flotation cell (PA-ECF). The design of the experiments, the modeling, and the optimization of the PA-ECF conditions for the treatment of DO concentrate rich in Pb were explored using a central composite design (CCD) under response surface methodology (RSM). Therefore, the CCD-RSM was employed to optimize and study the effect of the independent variables, namely electrolysis time (5.85 min to 116.15 min) and current intensity (0.09 A to 2.91 A) on Pb removal. Optimal values of the process parameters were determined as an electrolysis time of 77.65 min and a current intensity of 0.9 A. In addition to Pb removal (97.8%), energy consumption, electrode mass-consumed material, and operating cost were estimated as 0.0025 kWh/m^3, 0.217 kg Al/m^3, and 0.423 USD/m^3, respectively. In addition, it was found that DO concentrate obtained from metallurgical wastewater can be recovered through PA-ECF (almost 94% Pb removal). This work demonstrated that the PA-ECF technique could became a viable process applicable in the treatment of DO concentrate containing Pb-rich for reuse.

Keywords: electrocoagulation–flotation process; perforated aluminum; feed solution; direct osmosis; response surface methodology

Citation: Moosazade, M.; Ashoori, R.; Moghimi, H.; Amani, M.A.; Frontistis, Z.; Taheri, R.A. Electrochemical Recovery to Overcome Direct Osmosis Concentrate-Bearing Lead: Optimization of Treatment Process via RSM-CCD. *Water* **2021**, *13*, 3136. https://doi.org/10.3390/w13213136

Academic Editor: Sergi Garcia-Segura

Received: 16 October 2021
Accepted: 3 November 2021
Published: 8 November 2021

1. Introduction

Currently, environmental pollution related to heavy metals increasingly concerns the research community due to industrial development [1,2]. Improper discharge of effluents containing hazardous heavy metals such as lead (Pb) to water bodies will pose irreparable risks to aquatic organisms and, therefore, humans [3,4]. Improper discharge of untreated industrial wastewater containing Pb such as paper printing, electroplating, pigments, ammunition, petrol, metal pleating, and metallurgy is one of the leading causes of water contamination [5,6]. As stated in the framework of the European water policy, Pb is listed as a priority substance due to its persistence, toxicity, and bioaccumulation. The threshold limit for the presence of Pb in water is 10 ng mL^{-1} according to the European Council Directive 98/83/EC[1], [7]. Lead can affect the reproductive system and many organs of

the human body, such as the liver and kidneys, and alter brain functions. On the other hand, prolonged exposure to Pb can cause induce sterility, abortion, and neonatal deaths. To address this issue, finding a suitable and cost-effective way to remove Pb (or reduce it to a legally acceptable level) from aquatic environments has become a global challenge [3,8,9].

Many technologies have been used to remove heavy metals from the aqueous medium, such as ion exchange [8,9], adsorption [10,11], biological [12,13], electrochemical [14,15], and membrane technology [16,17]. Among them, direct osmosis (DO) has received special attention in recent years. DO is an emerging membrane technology in water/wastewater treatment methods that has some merits including low energy requirements, reduced membrane fouling, easy cleaning, and low or no additional pressure is needed in contrast to that of pressure-driven membrane processes. Theoretically, DO membranes can afford the reduction in heavy metal ions, which are multivalent in nature [18,19]. The draw solution and the feed solution were separated by a semi-permeable membrane in DO treatment. Water penetrates from the feed solution with lower concentration to draw solution with higher concentration while the membrane rejects unwanted compounds. The required separation flux is the difference in the osmotic pressure between draw solution and feed solution [20,21]. Despite the good quality of the treated water in this process and the adequate efficiency, a large volume of DO concentrate must be either discharged or further treated to offer a safe or low-risk effluent [22,23]. Hence, with the treatment of the DO concentrate, a knowledge gap remains. Therefore, alternative keys for treating such solutions are required.

Regarding DO treatment, electrocoagulation–flotation (ECF) technology as a green electrochemical process offers several merits such as low investment, design simplicity, nonspecific method, amenability to automation, environmental versatility, and a low energy low maintenance requirement [24–26]. The basic unit of ECF comprises an immersed anode and cathode inside the treated solution mounted in an electrolytic chamber powered by a direct current power supply [27]. ECF treatment can be achieved through three main mechanisms, including (i) destabilization of suspensions, (ii) particles entrapment, and (iii) adsorption of pollutants, once an electric current is applied through the direct current power supply to the submerged electrodes in aqueous medium metal coagulants released by oxidation and dissolution of the sacrificial anodes. On the other hand, reduction occurs at the cathode, resulting in hydrogen gas released as bubbles [28–30]. Therefore, the metal/hydroxide ions generated at the anode act as coagulants, while the precipitated hydroxides remove pollutants by sweep coagulation [31]. The chemical reactions in ECF reactors are as follows [32]:

Anode:

$$M \rightarrow M^{n+} + ne^- \quad (1)$$

$$2H_2O \rightarrow 4H^+ + O_2 + 4e^- \quad (2)$$

Cathode:

$$nH_2O + ne^- \rightarrow nOH^- + \frac{n}{2}H_2 \quad (3)$$

$$M^{n+} + ne^- \rightarrow M \quad (4)$$

Bulk solution:

$$M^{n+} + nOH^- \rightarrow M(OH)_n \quad (5)$$

Response surface methodology (RSM) consists of a powerful statistical approach useful for analyzing modeling and optimization problems where a response is affected by multiple independent variables [33]. In addition, RSM contains significant features over traditional experimental methods, such as time and experimental error reduction, mathematical modeling, improvement, and optimization processes [34,35]. However, the RSM combination with central composite design (CCD) is a broadly used optimization technique to study different processes used for water purification [36]. Because water/wastewater treatment technologies are affected by different variables, the optimization of parameters is necessary to achieve maximum process efficiency. Indeed, in recent years, many works

have investigated the effect of different parameters and their interactions in process performance using RSM [37–41]. The primary aim of this work was to fill the knowledge gap for the treatment or reuse of DO concentrate containing Pb-rich using perforated aluminium electrodes mounted in the ECF cell (PA-ECF). Moreover, this research focuses on optimizing the critical factors of the ECF technology, namely current intensity and electrolysis time, using CCD. Finally, an experiment under optimum conditions was conducted on actual DO concentrate obtained from metallurgical wastewater to evaluate the efficacy of PA-ECF in the real field.

2. Materials and Methods

2.1. Direct Osmosis Concentrate Characteristics

A commercial direct osmosis (DO) membrane (Aquaporin Asia Pte. Ltd., Singapore) was used to separate the feed solution and the draw solution. DO concentrate was produced during a series of experiments. The DO concentrate possessed pH = 1.1, electrical conductivity = 0.063 S/m, and Pb = 69.3 mg/L. Because the draw solution containing salts invariably passed through the membrane and entered the feed solution in the DO process, the feed solution's amount of electrical conductivity increased. Correspondingly, electrical conductivity of the solution tested in the present work was high. On the one hand, ECF technique is a good means for treating wastewater containing high electrical conductivity. On the other hand, it has a great advantage to increase process efficiency and reduce energy consumption [42].

2.2. Perforated Aluminium–Electrocoagulation–Flotation (PA-ECF) Set Up

A schematic diagram for the DO concentrate obtained from FO process using PA-ECF technique for treatment is shown in Figure 1. The PA-ECF runs were conducted in a 0.5 L volume beaker equipped with a magnetic stirrer to supply uniform mixing during the experiment. The speed of stirrer was preserved at 250 rpm. The ECF cell was provided with four monopolar perforated aluminium electrodes arranged in parallel connection. The dimensions of the perforated aluminium electrodes included width, length, and depth as 65 mm, 95 mm, and 2 mm, respectively, which were placed vertically in the middle of the cell. A perforated plastic sheet of a 1 mm thickness separates the cathode and anode electrodes, connected to a direct current power supply (0–30 V and 0–3 A).

After each assay, the treated samples were left to settle the precipitates produced from the ECF cell for 60 min. Then, the treated water was pumped into a beaker. The conductivity, Pb, and pH were measured. The perforated aluminium electrodes were regularly rubbed with abrasive paper before each ECF run and simultaneously rinsed with a mixture of acid reagent and distilled water to prevent electrode passivation.

2.3. Analytical Methods

According to Standard Methods for the Examination of Water and Wastewater, the amount of Pb solution was measured at 620 nm using a flame atomic absorption spectrophotometer (Rayleigh Analytical Instrument Corporation, WFX-130, Beijing, China) 3113 [43]. The pH of the solution was monitored using a pH meter (CONSORT C831, Hertenstraat, Belgium), while conductivity measurements were performed using a conductivity meter (Leybold GmbH 666222, Hürth, Germany).

The efficiency of Pb removal (R) (%) was estimated as follows [44]:

$$\% \text{ Pb removal} = ((C_0 - C_t)/C_0) \times 100 \quad (6)$$

where C_0 and C_t are the initial and final Pb concentration, respectively (mg/L).

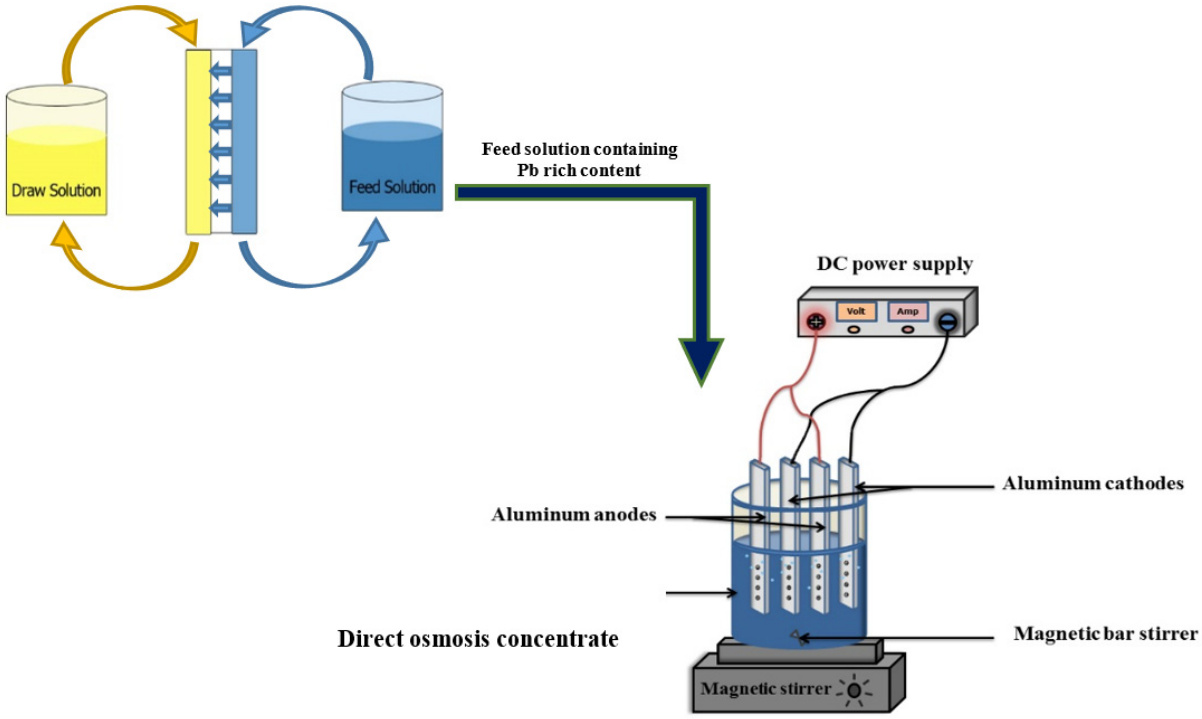

Figure 1. Schematic of the PA-ECF technique to treat DO concentrate containing Pb-rich.

2.4. Experimental Statistical Design

One of the powerful techniques used in mathematical modeling, design, and optimization of experimental conditions is the response level methodology (RSM). Compared to conventional methods, RSM reduces the time and costs of the test and thus significantly decreases test errors [33]. In the current work, RSM was employed in modeling and optimizing two variables: electrolysis time, current, and their interactions, while the response was the Pb removal efficiency. The experiments were designed and analyzed by the software Design Expert 7 (Stat-Ease, Inc., Minneapolis, MN, USA) using the central composite design (CCD). A set of 13 assays was codified for optimization based on two independent variables, including current value and electrolysis time through five levels. The domain of independent variables was controlled according to the values offered in the literature, and after obtaining the pre-test results [44,45], the coded critical factors are listed in Table 1. The system behavior was defined by second order polynomial Equation (7) [17]:

$$y\ (\%) = \beta_0 + \sum_{i=1}^{k} \beta_i X_i + \sum_{i=1}^{k} \beta_{ii} X_i^2 + \sum_{1 \le i \le j}^{k} \beta_{ij} X_i X_j + \varepsilon \quad (7)$$

where y denotes the response; i, j, and β_0 the linear constant, the second-order, and the constant coefficient, respectively. The regression constant, quadratic coefficient, and the interaction coefficient are β_i, β_{ii}, and β_{ij}, respectively. x_i and x_j are the coded independent variables.

Table 1. Experimental domain of CCD.

Independent	Code	Code Levels				
Variables	**Variables**	**−1.41**	**−1**	**0**	**+1**	**+1.41**
Electrolysis time (min)	A	5.85	22	61	100	116.15
Current intensity (A)	B	0.09	0.5	1.5	2.5	2.91

3. Results and Discussion

3.1. Modeling and Statistical Analysis via Central Composite Design (CCD)

The removal of contaminants from wastewater is highly dependent on the amount of metal ions released through the applied current during the ECF treatment time. Faraday's law is used as a simple relationship for an amount of electrode material dissolved. Consequently, the two crucial parameters for optimizing the pollutants removal in the ECF technique are the current intensity and electrolysis time. Setting them up to the optimal level can help reduce energy consumption and thus reduce operating costs [42]. Therefore, the CCD was used to define the effect of both individual parameters (electrolysis time and current intensity) and their interactions with the response variable (% Pb removal). Table 2 shows a total of 13 trials of Pb removal by the ECF process along with the experimental data vs. the data predicted by the quadratic model.

Table 2. Design matrix of experiments and results of CCD.

Runs	Standard Run No.	Experimental Matrix		Removal Efficiency (%)	
				Pb	
		A	B	Actual	Predicted
1	12	0	0	98.90	98.2
2	13	0	0	97.51	98.2
3	11	0	0	96.4	98.2
4	5	−1.41	0	92.89	92.72
5	10	0	0	99.87	98.2
6	2	+1	−1	91.53	91.75
7	7	0	−1.41	88.45	88.13
8	3	−1	+1	95.35	95.36
9	4	+1	+1	100.00	99.92
10	6	+1.41	0	97.64	97.59
11	9	0	0	98.31	98.2
12	1	−1	−1	89.12	89.42
13	8	0	+1.41	97.99	98.08

In Table 3, the predicted values were fitted with the second-order polynomial functions, where Υ_1 is Pb removal (%), and A, B are the electrolysis time and current intensity values, respectively. The negative sign reveals the antagonistic effects, while the positive sign reveals the synergistic effects. As shown in Table 4, analysis of variance (ANOVA) was used to attest to the adequacy of the model. The data illustrate a good fit between the quadratic model and the experimental data, with a relatively high R^2 of 0.96. The significant factors were ranked according to the *F*-value or *p*-value with 95% confidence level. The larger *F*-value 34.48 and the smaller '*p*' value (<0.0001) indicate that the model is significant. The lack of fit *F*-test describes the deviation of experimental data around the model. The lack of fit would not be significant as long as the model fits in well with the data. Table 5 shows that the lack of fit for the obtained model for Pb removal efficiency was not statistically significant, indicating weak model noise over their signal. Moreover, the model terms are significant only when the values of "Prob. > *F*" are less than 0.05. In this respect, electrolysis time (A), the quadratic terms of electrolysis time (A^2), and the quadratic terms of current intensity (B^2) have significant effects ($p < 0.05$), and current intensity (B) has a very significant effect ($p < 0.0001$) on Pb removal efficiency.

Table 3. The quadratic models for predicting responses of DO concentrate using the PA-ECF process.

Parameter	Equation for Real Variables
Υ_1 (Pb removal efficiency, %)	$+98.20 + 1.72 \times A + 3.52 \times B + 0.56 \times AB - 1.52 \times A^2 - 2.55 \times B^2$

A: electrolysis time; B: current intensity.

Table 4. ANOVA results of experiment data for Pb removal.

Source of Variations	Sum of Squares	Df	Mean Square	*F*-Value	*p*-Value Prob > *F*	Remarks
Model	179.67	5	35.93	34.48	<0.0001	Highly significant
A-Electrolysis time	23.73	1	23.73	22.77	0.002	significant
B-Current intensity	99.36	1	99.36	95.34	<0.0001	Highly significant
AB	1.25	1	1.25	1.20	0.3089	
A^2	16.15	1	16.15	15.50	0.0056	Significant
B^2	45.23	1	45.23	43.41	0.0003	Significant
Residual	7.29	7	1.04			
Lack of Fit	0.29	3	0.096	0.055	0.9809	Not significant
Pure Error	7.01	4	1.75			
Cor Total	186.97	12				
R^2/R^2_{adj} (%) = 0.96/0.93						

Different diagnostics tests were performed to examine the model validation and the graphical results are shown in Figure 2. Four aspects of graphical model validation are (I) normal probability plot of residuals (Figure 2a), (II) externally studentized residuals vs. predicted (Figure 2b), (III) externally studentized residuals vs. run number (Figure 2c), and (IV) predicted vs. actual plots (Figure 2d). The residuals as shown in Figure 2a lie near to the normal probability line, indicating that the model is reliable. Likewise, the plots of residuals (Figure 2b,c) depict that the residuals lie well within the acceptable range, further augmenting the model validation. Ultimately, it can be deduced from Figure 2d that the actual data comparatively overlap with the simulated data, which verifies that the model can be used for accurate predictions.

3.2. Importance of Influencing Parameters via Pareto Diagram Analysis

A Pareto diagram is a prevailing tool that describes the effect of each of the independent variables on the response acquired as the ratio of the pure sum (S_A) of each factor divided by the total sum of squares (SS_T) as stated in Equation (8). The significance of the applied current and treatment time is confirmed by the Pareto diagram illustrated in Figure 3 [46].

$$P_i\ (\%) = \frac{S_A}{SS_T} \tag{8}$$

According to the diagram, as presented in Figure 3, the electrolysis time and current intensity had the percent contributions of 53.14% and 12.69%, respectively, with a cumulative percentage of 65.83%. In conclusion, the current intensity was the crucial parameter rather than electrolysis time for Pb removal efficiency.

3.3. Interaction of Time and Current on Pb Removal

Figure 4a,b depicted the counter and 3D response surface plots of the effect of current and treatment time on Pb. Both the current intensity and electrolysis time are the utmost essential parameters in the ECF since the current determines the concentration of coagulants and the mixing. On the other hand, the electrolysis time determines the dissolution of aluminum ions (Al^{3+}), which strongly depends on the current value [47]. As shown, higher current intensity and electrolysis time achieved higher Pb removal. In addition, in agreement with Tables 3 and 4, the effect of current intensity on Pb removal is higher than electrolysis time. At the beginning of the PA-ECF process, the Pb removal diminished (blue region) due to a low pH of 1.5. However, the current study exhibited that the percentage of Pb removal is desirable (90%) even at low pH if the electrolysis time is long enough

(30 min), strictly in line with the literature [3,4]. It could be remarked that the greater the value of current and time of treatment, the greater the rate of the Pb abatement. In the red region on the plots, it is considered that the Pb removal reached a peak (entirely 100%) when the current increased to 2 A at 85 min of electrolysis time and pH reached approximately 5.5, then remained virtually constant at current intensity higher than 2 A. It is apparent that Al (III) in the form of Al $(OH)_3$(s) is the predominant species within pH range of 5.5–8.5 [48]. According to Faraday's law (Equation (11)), the mass of the electrode dissolved in the PA-ECF cell is proportional to the applied current. As is evident, at a more elevated current, the amplified generation of gas bubbles and coagulants increased the removal of contaminants through sedimentation or flotation [42,49]. However, since the consumption of both energy and electrodes increases with increasing applied current, very high current intensities are not desirable. Niazmand et al. [44] demonstrated that the highest removal of total phenolic compounds was observed at the highest current and time. Ait Ouaissa et al. [50] investigated the efficiency of an electrocoagulation unit with Al alloy in the removal of Cr (VI). According to their results, almost 97% of Cr (VI) was removed at a current density of 40 A/m^2 and an initial pH of 3 to 6.

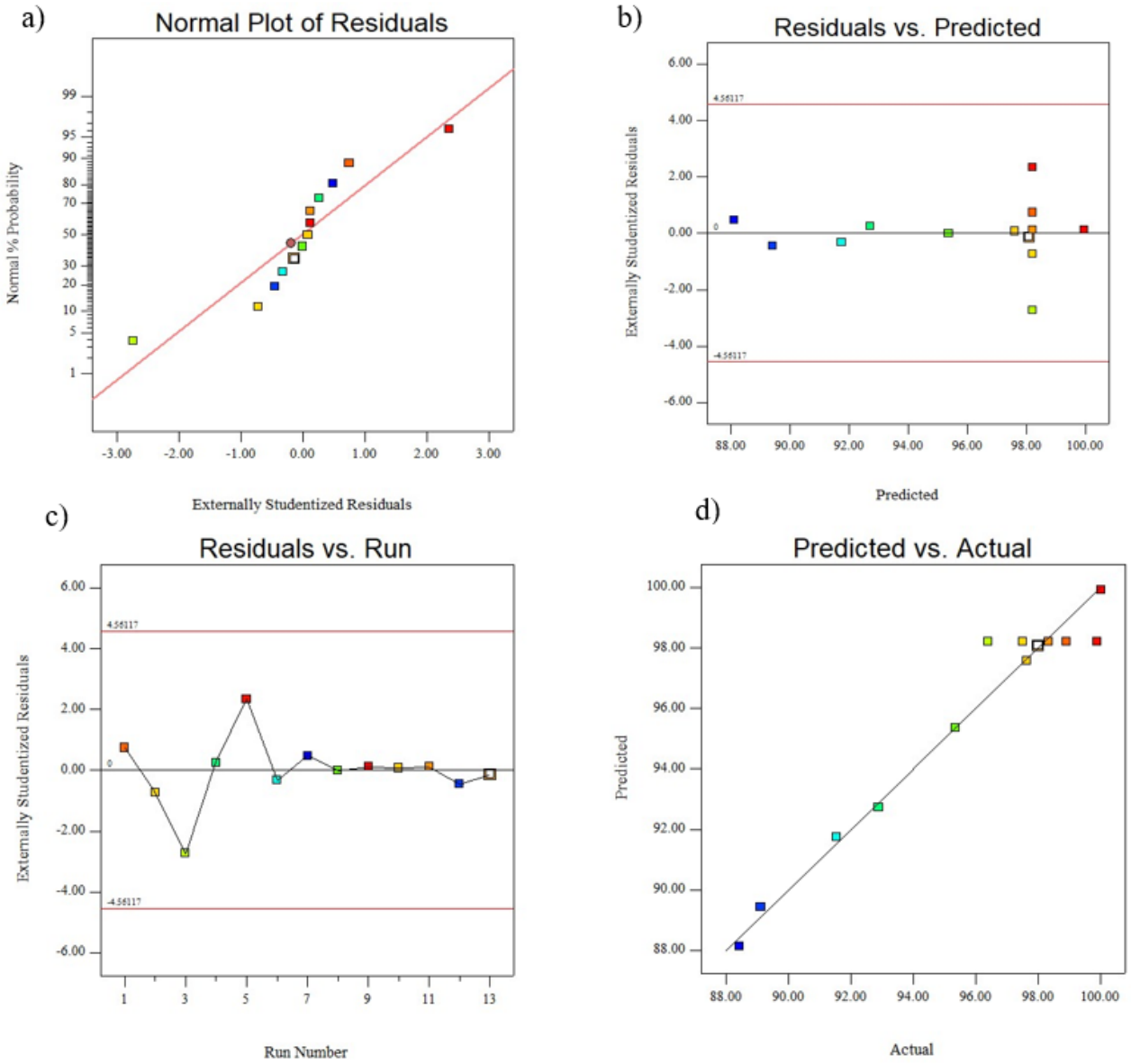

Figure 2. The normal probability plot of residuals (**a**), externally studentized residuals vs. predicted (**b**), externally studentized residuals vs. the run number (**c**), and predicted vs. actual plots (**d**) for Pb removal.

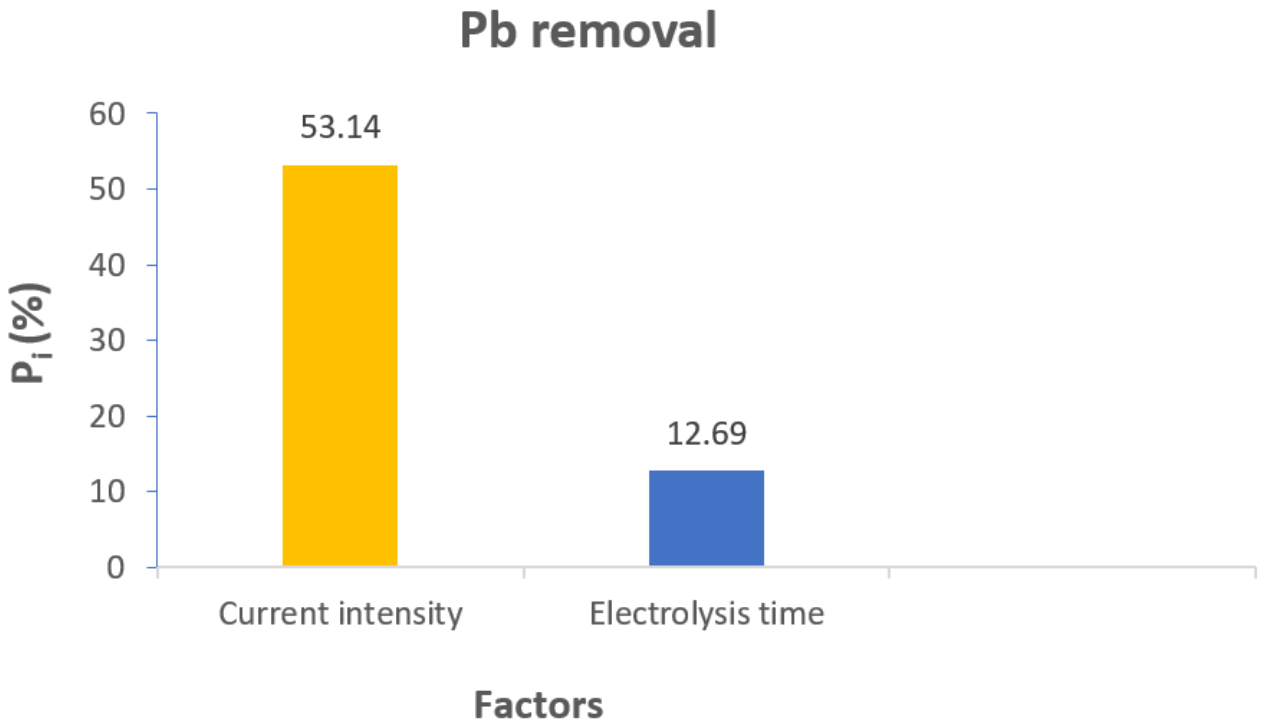

Figure 3. Pareto analysis of the effects of factors on Pb removal for DO concentrate treatment by the PA-ECF technique.

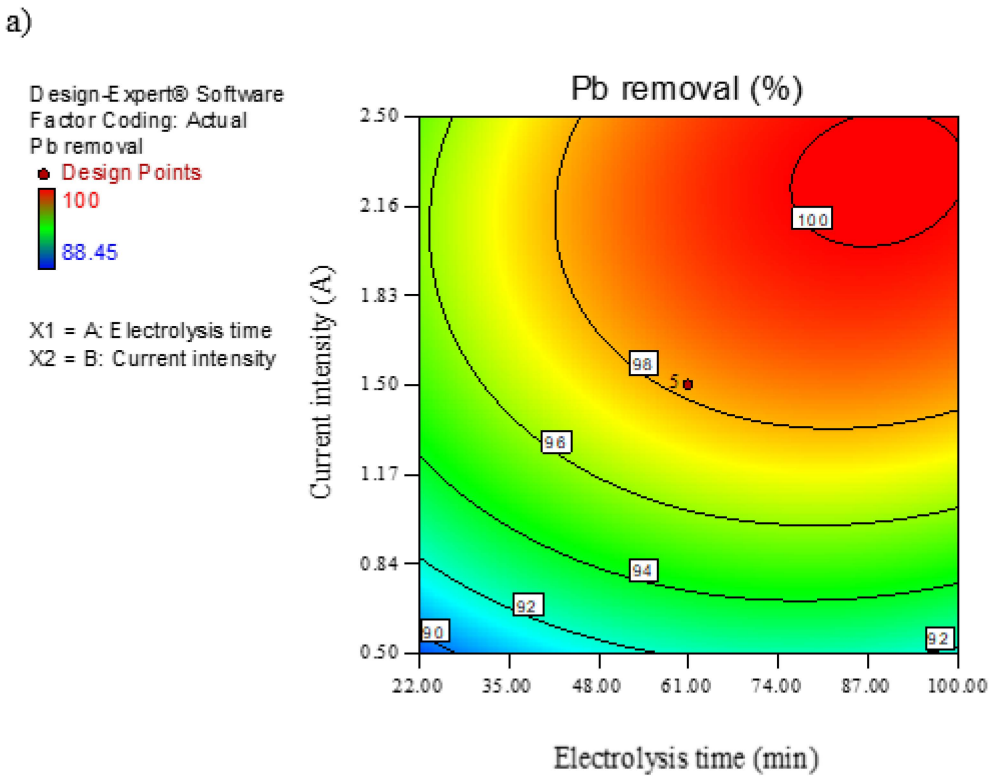

Figure 4. *Cont.*

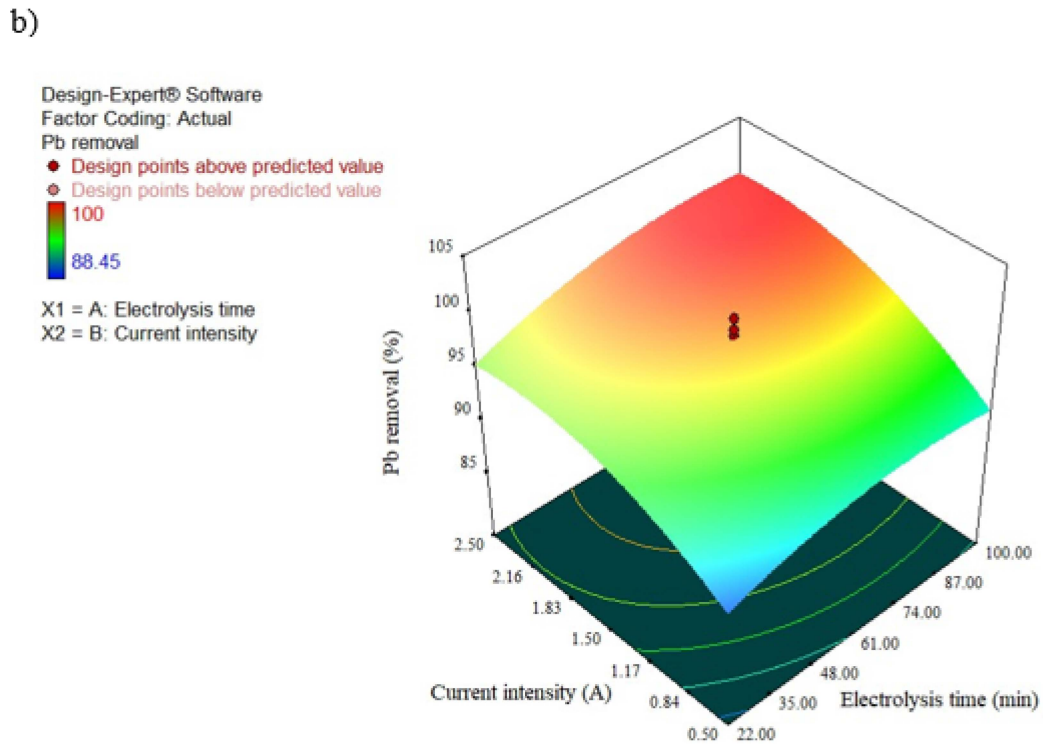

Figure 4. Contour plot (**a**), and 3D response surface plot (**b**) of the effect of current intensity and electrolysis time on removal efficiency of Pb.

3.4. Optimization Process

After analyzing the effect of the independent variables, a critical step is the use of the obtained model to optimize the target variables and maximize the response and, therefore, the Pb removal. In this context, when the independent variables were within the specified range in Table 2, as depicted in Figure 5, the higher Pb removal was estimated equal to 95.52%. According to the results of Table 5, the optimal conditions were estimated equal to 77.65 min of electrolysis and 0.9 A of current. An additional experiment under optimal conditions exhibited that the Pb removal efficiency (97.8%) and the predicted values were close to each other, indicating the model optimization's accuracy and validity. According to the literature, the RSM has been used to optimize the electrocoagulation treatment of various pollutants in recent years. For instance, Barışçı et al. [51] used the Box–Behnken design to examine the efficiency of the electrocoagulation process. After the optimization, they achieved lead removal (99%) at pH 5, using 26 A/m^2 and 0.5 g/L of electrolyte. Yoosefian et al. [52] reported optimization of iron–electrocoagulation treatment for ciprofloxacin antibiotic removal by RSM and CCD. Under optimal conditions (pH 7.5, a reaction time of 20 min, 150 A/m^2, and 1.5 cm interelectrode distance, the researchers achieved 99% CP removal. In the study of Genawi et al. [53] the researchers reported almost 100% electrocoagulation efficiency for the removal of Cr (VI) from tannery wastewater using RSM using 130 A/m^2 and pH 7.

On the other hand, Assadi et al. [8] used the Box–Behnken design for optimizing the Pb removal from wastewater using Al–electrocoagulation treatment. The removal approached 94% at optimal values: (pH 7.25 and 33 A/m^2). Furthermore, Ano et al. [54] analyzed nitrate removal by electrocoagulation using the Box–Behnken design under RSM. They found that under optimal conditions (1.80 A, 33 min, and pH 8.73), the nitrate removal was 73.8%.

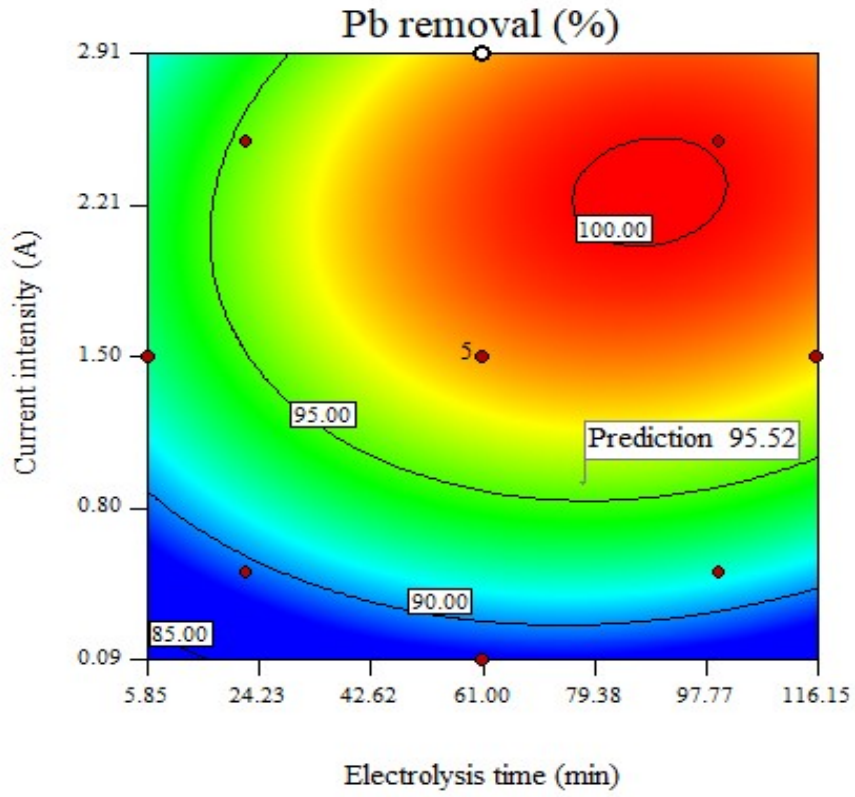

Figure 5. Contour plot of electrolysis time and current intensity on Pb removal at optimum condition.

Table 5. Optimal condition and comparison between actual value and predicted value.

Parameters	Electrolysis Time (min)	Current Intensity (A)	Removal (%) Predict	Removal (%) Experimental
Optimal value	77.65	0.9	97.8	95.52

3.5. Cost-Effectiveness Estimation

From an economic perspective, the mass of the sacrificed electrode and the energy consumed are major operating cost items of the ECF process. The electrochemical process of applying an electric current to the wastewater depends on the released different ions, which leads to the consumption of electrodes, so it is crucial to evaluate the operating cost of the reactor according to Equation (9) [55]:

$$\text{Operation cost} = \alpha \times M_{AEC} + \beta \times E_{CONS} \quad (9)$$

where M_{AEC} (kg/m^3) and E_{CONS} (kWh/m^3) are electrode mass-consumed material and energy required to remove the target contaminant, respectively; the Energy Ministry and Markets of Iran announced the prices of 1 kWh of electricity (α) and electrode material (β) as 0.04 USD/kWh and 1.95 USD/kg of Al in 2020, respectively.

The consumption of electrical energy (E_{CONS}) can be estimated by Equation (10), while the cost of electrodes is calculated by Faraday's law, which is influenced by time and current as Equation (11) [37]:

$$E_{CONS}\left(\frac{kWh}{m^3}\right) = \frac{U \times I \times T}{V_L} \quad (10)$$

$$M_{AEC}\left(\frac{kgFe}{m^3}\right) = \frac{I \times T \times MV}{Z \times F \times V_L} \quad (11)$$

U, I, T, and V_L denote the voltage applied (V), current (A), electrolysis time (h), and working volume (m^3), respectively. MV is the molecular mass of Al (26.98 g/mol), Z is the number of transferred electrons number (3), and F is the Faraday's constant (96,487 C/mol). Therefore, according to Equations (10) and (11), both energy and electrode consumptions were calculated to evaluate the operating cost of the cell (Equation (9)).

Finally, the operating treatment cost was defined in all runs planned by CCD-RSM. Figure 6 displays that the operation cost has an increasing trend for increased removal efficiency. For almost 100% Pb removal observed in run #9, the maximum operating cost was estimated as 0.1 USD/m^3. Under the optimal operating conditions, the necessary energy, the electrode mass, and the operating cost were equal to 0.0025 kWh/m^3, 0.217 kg Al/m^3, and 0.423 USD/m^3, respectively. Gonder et al. [56] estimated the total operating cost equal to 0.3 USD/m^3 using electrocoagulation-Al electrodes to remove organics, oil-grease, and chloride under optimum conditions (pH 6, 10 A/m^2, and 30 min). Bakshi et al. [57] applied electrocoagulation for phosphate removal, and the calculated operating cost was 0.22 USD/m^3 at optimized conditions (pH 7, 11.5 V, interelectrode distance of 3 cm, 0.5 kg/m^3 of salts, and 14 min of treatment). While, in another study, Bian et al. [58] reported energy consumption between 0.378 and 0.977 kWh/m^3 to treat oily bilge using electrocoagulation, which was much higher than the value of the present study. As the results revealed, the present study confirms previous findings.

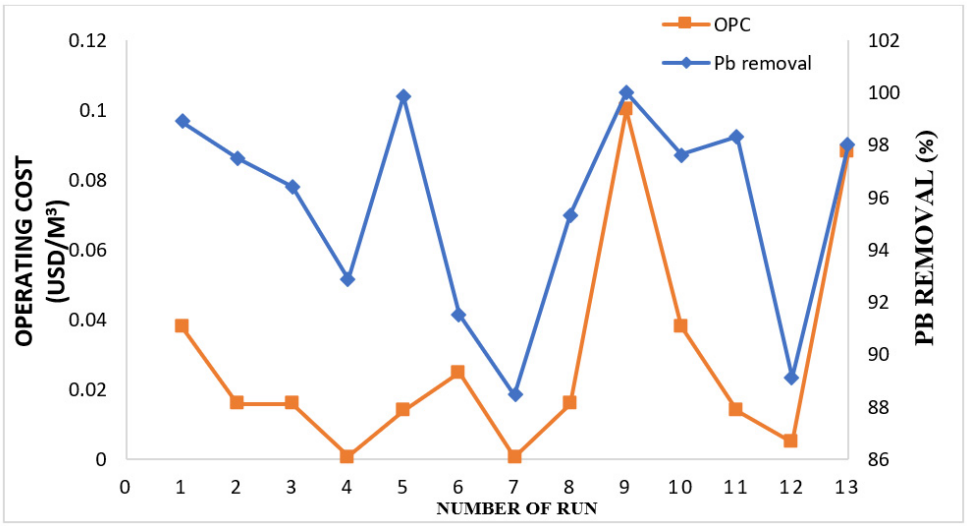

Figure 6. The operating cost vs. Pb removal through 13 experiments designed by CCD-RSM.

3.6. Treatment of Direct Osmosis Concentrate from Metallurgical Industry

The metallurgical industry is one of the major industries producing heavy metals, especially Pb. In addition, the industry discharges considerable amounts of wastewater into the aquatic environment, which is dangerous for human and living organisms and leads to altering the functioning of organs. In this study, metallurgical wastewater was used as a potential source of Pb to estimate the efficiency of the proposed process to treat DO concentrate in the actual field.

In agreement with the synthetic solutions treated previously, a direct osmosis process was applied to obtain DO concentrate from metallurgical wastewater. After performing the assays, the DO concentrate had pH 3.5, contained 98.2 mg/L of Pb (as a target pollutant), and the electrical conductivity was 0.041 S/m. Therefore, a perforated aluminum electrocoagulation–flotation (PA-ECF) experiment was conducted using the optimal conditions obtained in the previous section (electrolysis time of 77.65 min and current intensity of 0.9 A). In the same vein, at the optimal point, five series of experiments were performed under the same conditions (Figure 7), which resulted in an average of 94.2% Pb removal from DO concentrate of the actual metallurgical wastewater. As a result, it was found

that the PA-ECF process can be used as an economically viable solution to solve the DO concentrate membrane challenge.

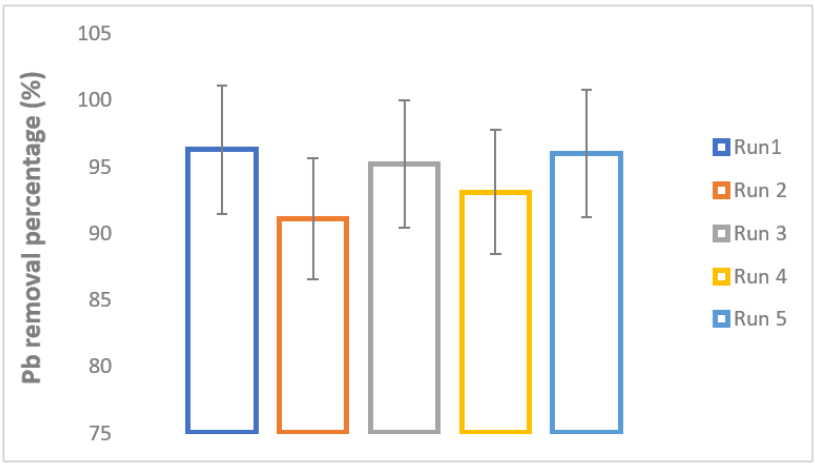

Figure 7. A set of experiments under optimal conditions (electrolysis time of 77.65 min and current intensity of 0.9 A) for Pb removal from DO concentrate of the actual metallurgical wastewater.

4. Conclusions

To summarize, the ECF process using perforated aluminum electrodes (PA-ECF) would cope with DO concentrate, a major membrane challenge, containing Pb-rich produced from the feed solution. The CCD-RSM was used successfully as a statistical tool, which reduces the number of trials and optimizes the operating factors. According to the Pareto analysis, the current intensity had a more significant impact on Pb removal efficiency rather than treatment time with contributions of 53.14% and 12.69%, respectively. Under optimal conditions (electrolysis time of 77.65 min and current intensity of 0.9 A), the Pb removal, the energy consumed, the electrode mass-consumed material, and the operating cost were estimated equal to 97.8%, 0.0025 kWh/m^3, 0.217 kg Al/m^3, and 0.423 USD/m^3. It can be concluded that modeling and optimization by CCD under RSM could lead to satisfactory results. In addition, 94.2% Pb removal was achieved from DO concentrate of real metallurgical wastewater through PA-ECF. Although the prospect of this study was to examine the process on an industrial scale and to achieve reasonable results with real operating parameters, further studies are essential to examine electrochemical degradation pathways and mechanisms for Pb removal via GC-MS analysis.

Author Contributions: Conceptualization, methodology, formal analysis, data curation, investigation, writing—original draft, project administration, M.M.; visualization, software, validation, investigation, data curation, writing—original draft, R.A.; writing—review and editing, H.M., M.A.A., and Z.F.; resources, supervision, writing—review and editing, R.A.T. All authors have read and agreed to the published version of the manuscript.

Funding: This research did not receive any specific grant from funding agencies in the public, commercial, or not-for-profit sectors.

Institutional Review Board Statement: Not applicable.

Informed Consent Statement: Not applicable.

Data Availability Statement: The authors confirm that the data supporting the findings of this study are available within the article.

Acknowledgments: The authors would like to thank from the "Clinical Research Development Center of Baqiyatallah hospital" for their kind cooperation.

Conflicts of Interest: The authors declare no conflict of interest.

References

1. Fallah, S.; Mamaghani, H.R.; Yegani, R.; Hajinajaf, N.; Pourabbas, B. Use of graphene substrates for wastewater treatment of textile industries. *Adv. Compos. Hybrid Mater.* **2020**, *3*, 187–193. [CrossRef]
2. Kinuthia, G.K.; Ngure, V.; Beti, D.; Lugalia, R.; Wangila, A.; Kamau, L. Levels of heavy metals in wastewater and soil samples from open drainage channels in Nairobi, Kenya: Community health implication. *Sci. Rep.* **2020**, *10*, 8434. [CrossRef]
3. Bouguerra, W.; Barhoumi, A.; Ibrahim, N.; Brahmi, K.; Aloui, L.; Hamrouni, B. Optimization of the electrocoagulation process for the removal of lead from water using aluminium as electrode material. *Desalination Water Treat.* **2015**, *56*, 2672–2681. [CrossRef]
4. Escobar, C.; Soto-Salazar, C.; Toral, M.I. Optimization of the electrocoagulation process for the removal of copper, lead and cadmium in natural waters and simulated wastewater. *J. Environ. Manag.* **2006**, *81*, 384–391. [CrossRef]
5. Ahmad, N.; Sereshti, H.; Mousazadeh, M.; Nodeh, H.R.; Kamboh, M.A.; Mohamad, S. New magnetic silica-based hybrid organic-inorganic nanocomposite for the removal of lead (II) and nickel (II) ions from aqueous solutions. *Mater. Chem. Phys.* **2019**, *226*, 73–81. [CrossRef]
6. Pohl, A. Removal of heavy metal ions from water and wastewaters by sulfur-containing precipitation agents. *Water Air Soil Pollut.* **2020**, *231*, 503. [CrossRef]
7. EU, European Community. Council Directive 98/83/EC of 3 November 1998 on the quality of water intended for human consumption. *Off. J. Eur. Communities* **1998**, 32–54. Available online: https://eur-lex.europa.eu/legal-content/EN/TXT/?uri=celex%3A31998L0083 (accessed on 18 October 2021).
8. Assadi, A.; Fazli, M.M.; Emamjomeh, M.M.; Ghasemi, M. Optimization of lead removal by electrocoagulation from aqueous solution using response surface methodology. *Desalination Water Treat.* **2016**, *57*, 9375–9382. [CrossRef]
9. Mansoorian, H.J.; Mahvi, A.H.; Jafari, A.J. Removal of lead and zinc from battery industry wastewater using electrocoagulation process: Influence of direct and alternating current by using iron and stainless steel rod electrodes. *Sep. Purif. Technol.* **2014**, *135*, 165–175. [CrossRef]
10. Lai, Y.-C.; Chang, Y.-R.; Chen, M.-L.; Lo, Y.-K.; Lai, J.-Y.; Lee, D.-J. Poly (vinyl alcohol) and alginate cross-linked matrix with immobilized Prussian blue and ion exchange resin for cesium removal from waters. *Bioresour. Technol.* **2016**, *214*, 192–198. [CrossRef]
11. Verma, V.; Tewari, S.; Rai, J. Ion exchange during heavy metal bio-sorption from aqueous solution by dried biomass of macrophytes. *Bioresour. Technol.* **2008**, *99*, 1932–1938. [CrossRef] [PubMed]
12. Cochrane, E.; Lu, S.; Gibb, S.; Villaescusa, I. A comparison of low-cost biosorbents and commercial sorbents for the removal of copper from aqueous media. *J. Hazard. Mater.* **2006**, *137*, 198–206. [CrossRef]
13. Davarnejad, R.; Panahi, P. Cu (II) removal from aqueous wastewaters by adsorption on the modified Henna with Fe3O4 nanoparticles using response surface methodology. *Sep. Purif. Technol.* **2016**, *158*, 286–292. [CrossRef]
14. Javid, A.B.; Barzanouni, H.; Younesi, A.; Amir, N.; Farahani, A.; Mousazadeh, M.; Soleimani, P. Performance of modified one-stage Phoredox reactor with hydraulic up-flow in biological removal of phosphorus from municipal wastewater. *Desalination Water Treat.* **2019**, *171*, 216–222.
15. Sierra-Alvarez, R.; Karri, S.; Freeman, S.; Field, J.A. Biological treatment of heavy metals in acid mine drainage using sulfate reducing bioreactors. *Water Sci. Technol.* **2006**, *54*, 179–185. [CrossRef] [PubMed]
16. Akbal, F.; Camcı, S. Copper, chromium and nickel removal from metal plating wastewater by electrocoagulation. *Desalination* **2011**, *269*, 214–222. [CrossRef]
17. Dharnaik, A.S.; Ghosh, P.K. Hexavalent chromium [Cr (VI)] removal by the electrochemical ion-exchange process. *Environ. Technol.* **2014**, *35*, 2272–2279. [CrossRef]
18. Mohsen-Nia, M.; Montazeri, P.; Modarress, H. Removal of Cu^{2+} and Ni^{2+} from wastewater with a chelating agent and reverse osmosis processes. *Desalination* **2007**, *217*, 276–281. [CrossRef]
19. Naghdali, Z.; Sahebi, S.; Ghanbari, R.; Mousazadeh, M.; Ali Jamali, H. Chromium removal and water recycling from electroplating wastewater through direct osmosis: Modeling and optimization by response surface methodology. *Environ. Health Eng. Manag. J.* **2019**, *6*, 113–120. [CrossRef]
20. Li, Z.; Linares, R.V.; Bucs, S.; Fortunato, L.; Hélix-Nielsen, C.; Vrouwenvelder, J.S.; Ghaffour, N.; Leiknes, T.; Amy, G. Aquaporin based biomimetic membrane in forward osmosis: Chemical cleaning resistance and practical operation. *Desalination* **2017**, *420*, 208–215. [CrossRef]
21. Naghdali, Z.; Sahebi, S.; Mousazadeh, M.; Jamali, H.A. Optimization of the forward osmosis process using aquaporin membranes in chromium removal. *Chem. Eng. Technol.* **2020**, *43*, 298–306. [CrossRef]
22. Cui, Y.; Ge, Q.; Liu, X.-Y.; Chung, T.-S. Novel forward osmosis process to effectively remove heavy metal ions. *J. Membr. Sci.* **2014**, *467*, 188–194. [CrossRef]
23. Mi, B.; Elimelech, M. Gypsum scaling and cleaning in forward osmosis: Measurements and mechanisms. *Environ. Sci. Technol.* **2010**, *44*, 2022–2028. [CrossRef]
24. Labiadh, L.; Fernandes, A.; Ciríaco, L.; Pacheco, M.J.; Gadri, A.; Ammar, S.; Lopes, A. Electrochemical treatment of concentrate from reverse osmosis of sanitary landfill leachate. *J. Environ. Manag.* **2016**, *181*, 515–521. [CrossRef]
25. Renou, S.; Givaudan, J.; Poulain, S.; Dirassouyan, F.; Moulin, P. Landfill leachate treatment: Review and opportunity. *J. Hazard. Mater.* **2008**, *150*, 468–493. [CrossRef]

26. Emamjomeh, M.M.; Jamali, H.A.; Naghdali, Z.; Mousazadeh, M. Efficiency of Electrocoagulation, Sedimentation and Filtration Hybrid Process in Removing Chemical Oxygen Demand and Turbidity from Carwash Industrial Wastewater: Optimization by Response Surface Methodology. *J. Maz. Univ. Med. Sci.* **2019**, *29*, 106–120.
27. Kabdaşlı, I.; Arslan-Alaton, I.; Ölmez-Hancı, T.; Tünay, O. Electrocoagulation applications for industrial wastewaters: A critical review. *Environ. Technol. Rev.* **2012**, *1*, 2–45. [CrossRef]
28. Mousazadeh, M.; Alizadeh, S.; Frontistis, Z.; Kabdaşlı, I.; Karamati Niaragh, E.; Al Qodah, Z.; Naghdali, Z.; Mahmoud, A.E.D.; Sandoval, M.A.; Butler, E. Electrocoagulation as a Promising Defluoridation Technology from Water: A Review of State of the Art of Removal Mechanisms and Performance Trends. *Water* **2021**, *13*, 656. [CrossRef]
29. Titchou, F.E.; Zazou, H.; Afanga, H.; El Gaayda, J.; Akbour, R.A.; Nidheesh, P.V.; Hamdani, M. An overview on the elimination of organic contaminants from aqueous systems using electrochemical advanced oxidation processes. *J. Water Process Eng.* **2021**, *41*, 102040. [CrossRef]
30. Afanga, H.; Zazou, H.; Titchou, F.E.; Rakhila, Y.; Akbour, R.A.; Elmchaouri, A.; Ghanbaja, J.; Hamdani, M. Integrated electrochemical processes for textile industry wastewater treatment: System performances and sludge settling characteristics. *Sustain. Environ. Res.* **2020**, *30*, 1–11. [CrossRef]
31. Emamjomeh, M.; Kakavand, S.; Jamali, H.; Alizadeh, S.; Safdari, M.; Mousavi, S.E.S.; Hashim, K.S.; Mousazadeh, M. The treatment of printing and packaging wastewater by electrocoagulation–flotation: The simultaneous efficacy of critical parameters and economics. *Desalination Water Treat.* **2020**, *205*, 161–174. [CrossRef]
32. Emamjomeh, M.M.; Jamali, H.A.; Naghdali, Z.; Mousazadeh, M. Carwash wastewater treatment by the application of an environmentally friendly hybrid system: An experimental design approach. *Desalination Water Treat.* **2019**, *160*, 171–177. [CrossRef]
33. Bazrafshan, E.; Mohammadi, L.; Ansari-Moghaddam, A.; Mahvi, A.H. Heavy metals removal from aqueous environments by electrocoagulation process—A systematic review. *J. Environ. Health Sci. Eng.* **2015**, *13*, 74. [CrossRef]
34. Titchou, F.E.; Afanga, H.; Zazou, H.; Akbour, R.A.; Hamdani, M. Batch elimination of cationic dye from aqueous solution by electrocoagulation process. *Mediterr. J. Chem.* **2020**, *10*, 1–12. [CrossRef]
35. Abdulgader, M.; Yu, Q.J.; Zinatizadeh, A.A.; Williams, P.; Rahimi, Z. Application of response surface methodology (RSM) for process analysis and optimization of milk processing wastewater treatment using multistage flexible fiber biofilm reactor. *J. Environ. Chem. Eng.* **2020**, *8*, 103797. [CrossRef]
36. Nair, A.T.; Makwana, A.R.; Ahammed, M.M. The use of response surface methodology for modelling and analysis of water and wastewater treatment processes: A review. *Water Sci. Technol.* **2014**, *69*, 464–478. [CrossRef]
37. Trinh, T.K.; Kang, L.S. Response surface methodological approach to optimize the coagulation–flocculation process in drinking water treatment. *Chem. Eng. Res. Des.* **2011**, *89*, 1126–1135. [CrossRef]
38. Pandey, N.; Thakur, C. Statistical Comparison of Response Surface Methodology–Based Central Composite Design and Hybrid Central Composite Design for Paper Mill Wastewater Treatment by Electrocoagulation. *Process Integr. Optim. Sustain.* **2020**, *4*, 343–359. [CrossRef]
39. Emamjomeh, M.M.; Mousazadeh, M.; Mokhtari, N.; Jamali, H.A.; Makkiabadi, M.; Naghdali, Z.; Hashim, K.S.; Ghanbari, R. Simultaneous removal of phenol and linear alkylbenzene sulfonate from automotive service station wastewater: Optimization of coupled electrochemical and physical processes. *Sep. Sci. Technol.* **2020**, *55*, 3184–3194. [CrossRef]
40. Khan, S.U.; Mahtab, M.S.; Farooqi, I.H. Enhanced lead (II) removal with low energy consumption in an electrocoagulation column employing concentric electrodes: Process optimisation by RSM using CCD. *Int. J. Environ. Anal. Chem.* **2021**, 1–18. [CrossRef]
41. Khanniri, E.; Yousefi, M.; Mortazavian, A.M.; Khorshidian, N.; Sohrabvandi, S.; Arab, M.; Koushki, M.R. Effective removal of lead (II) using chitosan and microbial adsorbents: Response surface methodology (RSM). *Int. J. Biol. Macromol.* **2021**, *178*, 53–62. [CrossRef] [PubMed]
42. Moghaddam, S.S.; Moghaddam, M.A.; Arami, M. Coagulation/flocculation process for dye removal using sludge from water treatment plant: Optimization through response surface methodology. *J. Hazard. Mater.* **2010**, *175*, 651–657. [CrossRef]
43. Mosaddeghi, M.R.; Pajoum Shariati, F.; Vaziri Yazdi, S.A.; Nabi Bidhendi, G. Application of response surface methodology (RSM) for optimizing coagulation process of paper recycling wastewater using Ocimum basilicum. *Environ. Technol.* **2020**, *41*, 100–108. [CrossRef] [PubMed]
44. Niazmand, R.; Jahani, M.; Sabbagh, F.; Rezania, S. Optimization of Electrocoagulation Conditions for the Purification of Table Olive Debittering Wastewater Using Response Surface Methodology. *Water* **2020**, *12*, 1687. [CrossRef]
45. APHA. *Standard Methods for the Examination of Water and Wastewater*; APHA American Public Health Association: Washington, DC, USA, 2003; Volume 2.
46. Khan, S.U.; Islam, D.T.; Farooqi, I.H.; Ayub, S.; Basheer, F. Hexavalent chromium removal in an electrocoagulation column reactor: Process optimization using CCD, adsorption kinetics and pH modulated sludge formation. *Process Saf. Environ. Prot.* **2019**, *122*, 118–130. [CrossRef]
47. Mousazadeh, M.; Naghdali, Z.; Al-Qodah, Z.; Alizadeh, S.; Niaragh, E.K.; Malekmohammadi, S.; Nidheesh, P.; Roberts, E.P.; Sillanpää, M.; Emamjomeh, M.M. A systematic diagnosis of state of the art in the use of electrocoagulation as a sustainable technology for pollutant treatment: An updated review. *Sustain. Energy Technol. Assess.* **2021**, *47*, 101353.
48. Gönder, Z.B.; Arayici, S.; Barlas, H. Treatment of pulp and paper mill wastewater using utrafiltration process: Optimization of the fouling and rejections. *Ind. Eng. Chem. Res.* **2012**, *51*, 6184–6195. [CrossRef]

49. Emamjomeh, M.M.; Sivakumar, M. An empirical model for defluoridation by batch monopolar electrocoagulation/flotation (ECF) process. *J. Hazard. Mater.* **2006**, *131*, 118–125. [CrossRef]
50. Ait Ouaissa, Y.; Chabani, M.; Amrane, A.; Bensmaili, A. Removal of Cr (VI) from model solutions by a combined electrocoagulation sorption process. *Chem. Eng. Technol.* **2013**, *36*, 147–155. [CrossRef]
51. Barışçı, S.; Turkay, O. Optimization and modelling using the response surface methodology (RSM) for ciprofloxacin removal by electrocoagulation. *Water Sci. Technol.* **2016**, *73*, 1673–1679. [CrossRef]
52. Yoosefian, M.; Ahmadzadeh, S.; Aghasi, M.; Dolatabadi, M. Optimization of electrocoagulation process for efficient removal of ciprofloxacin antibiotic using iron electrode; kinetic and isotherm studies of adsorption. *J. Mol. Liq.* **2017**, *225*, 544–553. [CrossRef]
53. Genawi, N.M.; Ibrahim, M.H.; El-Naas, M.H.; Alshaik, A.E. Chromium Removal from Tannery Wastewater by Electrocoagulation: Optimization and Sludge Characterization. *Water* **2020**, *12*, 1374. [CrossRef]
54. Ano, J.; Briton, B.G.H.; Kouassi, K.E.; Adouby, K. Nitrate removal by electrocoagulation process using experimental design methodology: A techno-economic optimization. *J. Environ. Chem. Eng.* **2020**, *8*, 104292. [CrossRef]
55. AlJaberi, F.Y. Operating cost analysis of a concentric aluminum tubes electrodes electrocoagulation reactor. *Heliyon* **2019**, *5*, e02307. [CrossRef] [PubMed]
56. Gönder, Z.B.; Balcıoğlu, G.; Vergili, I.; Kaya, Y. Electrochemical treatment of carwash wastewater using Fe and Al electrode: Techno-economic analysis and sludge characterization. *J. Environ. Manag.* **2017**, *200*, 380–390. [CrossRef]
57. Bakshi, A.; Verma, A.K.; Dash, A.K. Electrocoagulation for removal of phosphate from aqueous solution: Statistical modeling and techno-economic study. *J. Clean. Prod.* **2020**, *246*, 118988. [CrossRef]
58. Bian, Y.; Ge, Z.; Albano, C.; Lobo, F.L.; Ren, Z.J. Oily bilge water treatment using DC/AC powered electrocoagulation. *Environ. Sci. Water Res. Technol.* **2019**, *5*, 1654–1660. [CrossRef]